Low Temperature Catalytic Pyrolysis for the Synthesis of High Surface Area, Nanostructured Graphitic Carbon

An-Hui Lu,* Wen-Cui Li, Elena-Lorena Salabas, Bernd Spliethoff, and Ferdi Schüth

Max-Planck-Institut für Kohlenforschung, Kaiser-Wilhelm-Platz 1, D-45470 Mülheim an der Ruhr, Germany

Received January 19, 2006. Revised Manuscript Received February 28, 2006

High surface area graphitic carbons are of great interest in emerging applications including catalysis and energy storage because of the well-developed crystalline structure, high electronic conductivity and thermal stability, and satisfactory oxidation resistance at low temperature. We have developed the synthesis of porous graphitic carbon with a large and accessible surface area via synthesis of carboxyl-containing polymer particles, followed by ion exchange and pyrolysis at low temperature (850 °C). The evolution of the graphitic structure together with mesoporosity is temperature dependent, as revealed from the results of X-ray diffraction, transmission electron microscopy, and nitrogen sorption measurement. Specifically, the development of mesoporosity resulting from continuously catalyzed carbonization by the in situ formed cobalt nanoparticles can be clearly recognized. Further nitric acid oxidation leads to an increase of the pore volume due to the removal of cobalt nanoparticles and opening of closed pore entrances. Moreover, the use of silica as the isolating shell facilitates the formation of high surface area graphitic carbon. Magnetization measurements show that the graphitic carbon/cobalt composites exhibit ferromagnetic properties, and the cobalt nanoparticles are stable under air for more than 10 months without degradation of their magnetic properties.

1. Introduction

The discoveries of fullerenes and carbon nanotubes have triggered intense research on nanostructured carbon materials for possible applications as adsorbents, catalyst supports, electrode materials, and energy storage media.[1] Many studies have been published on the control of the nanostructures of porous carbons, including surface area, pore size, and nature of the carbon framework, to meet the particular requirements of specific applications.[2] For the intended application fields the properties of the carbon play a critical role in determining the performance of the systems. Specifically, porous graphitic carbon shows advantages over amorphous carbon because of the well-developed crystalline structure, high electronic conductivity and thermal stability, and satisfactory oxidation resistance at low temperature as well. Thus, the synthesis of porous graphitic carbon with a large and accessible surface area is of great interest in the applications listed above.

Nanostructured carbon materials with graphitic nature, including carbon nanotubes, carbon nanofibers, and carbon onions, are usually produced under harsh conditions, such as arc discharge, laser evaporation, and thermal chemical vapor deposition.[3] However, these synthetic methods have limitations in terms of scalability and economics because of the demanding synthetic conditions and generally low yields. Conventional methods for the preparation of graphitic carbon often require high temperature treatment. Although heat treatment at high temperature, normally higher than 2000 °C, is able to form porous carbon with well-developed graphitic order, such reaction conditions are rather energy- and capital-intensive; in addition, they lead to a significant reduction in the surface area and pore volume of the porous carbon.[4] Activation procedures, usually used to prepare activated carbons with high surface area, are not suitable for graphitizable carbons, because these carbons are difficult to penetrate for gasifying agents, which prevents the creation of pores. Consequently, the development of porosity is poor. Moreover, substantial mass loss takes place as a result of the layer-by-layer etching of graphite by the active agent.

Over the last years, several methods, basically involving the use of catalysts or high temperature treatment, were developed to synthesize porous graphitic carbons. Many groups have been working on metal-doped carbon aerogels for

* To whom correspondence should be addressed. Fax: +49-0208 306 2995. E-mail: lu@mpi-muelheim.mpg.de.

(1) (a) Iijima, S. *Nature* **1991**, *354*, 56. (b) Hu, J.; Ouyang, M.; Yang, P.; Lieber, C. M. *Nature* **1999**, *399*, 48. (c) Bessel, C. A.; Laubernds, K.; Rodriguez, N. M.; Baker, R. T. K. *J. Phys. Chem. B* **2001**, *105*, 1115. (d) Liang, C.; Li, Z.; Qiu, J.; Li, C. *J. Catal.* **2002**, *211*, 278.

(2) (a) Ryoo, R.; Joo, S. H.; Jun, S. *J. Phys. Chem. B* **1999**, *103*, 7743. (b) Lu, A.-H.; Schmidt, W.; Spliethoff, B.; Schüth, F. *Adv. Mater.* **2003**, *15*, 1602. (c) Lu, A.-H.; Kiefer, A. Schmidt, W.; Schüth, F. *Chem. Mater.* **2004**, *16*, 100. (d) Lu, A.-H.; Li, W.; Schmidt, W.; Kiefer, W.; Schüth, F. *Carbon* **2004**, *42*, 2939. (e) Lu, A.-H.; Schmidt, W.; Matoussevitch, N.; Bönnermann, H.; Spliethoff, B.; Tesche, B.; Bill, E.; Kiefer, W.; Schüth, F. *Angew. Chem., Int. Ed.* **2004**, *43*, 4303. (f) Lee, J.; Han, S.; Hyeon, T. *J. Mater. Chem.* **2004**, *14*, 478. (g) El Hamaoui, B.; Zhi, L.; Wu, J.; Kolb, U.; Müllen, K. *Adv. Mater.* **2005**, *17*, 2957.

(3) (a) Journet, C.; Master, W. K.; Bernier, P.; Loiseau, A.; Lamy de la Chapellw, M.; Lefrant, S.; Deniard, P.; Lee, R.; Fisher, J. E. *Nature* **1997**, *388*, 756. (b) Thess, A.; Lee, R; Nikolaev, P.; Dai, H. J.; Petit, P.; Robert, J.; Xu, C. H.; Lee, Y. H.; Kim, S. G.; Rinzler, A. G.; Colbert, D. T.; Scuseria, G. E.; Tomanek, D.; Fisher, J. E.; Smalley, R. E. *Science* **1996**, *273*, 483. (c) Terrones, M.; Grobert, N.; Olivares, J.; Zhang, J. P.; Terrones, H.; Kordatos, K.; Hsu, W. K.; Hare, J. P.; Townsend, P. D.; Prassides, K.; Cheetham, A. K.; Kroto, H. W.; Walton, D. R. M. *Nature* **1997**, *388*, 52.

(4) Hanzawa, Y.; Hatori, H.; Yoshizawa, N.; Yamada, Y. *Carbon* **2002**, *40*, 575.

10.1021/cm060135p CCC: $33.50
Published on Web 03/25/2006

catalysis, adsorption, and electrode materials.[5] For instance, after pyrolysis of supercritically dried carbon aerogels doped with cobalt or nickel at 1050 °C the growth of graphitic nanoribbons with different curvatures is observed.[6] By heating Cr-, Fe-, Co-, or Ni-doped carbon aerogels higher than 1000 °C, graphitized domains with three-dimensional stacking order can be formed in carbon aerogel.[7] By heat treating composites made up of resorcinol−formaldehyde gel, silica, and transition-metal salt, followed by washing with NaOH solution and HNO_3 solution to remove silica and metal particles, carbon nanocoils were generated.[8] We found that, by using cobalt nanoparticles as the sacrificial template and cetyltrimethylammonium bromide (CTAB) as the surfactant and carbon source, a graphitic hollow shell could be fabricated after pyrolysis at 850 °C and following leaching of the cobalt nanoparticles by acid solution.[9] Graphitized nanoporous carbon with spherical pores was prepared by graphitization at 2500 °C of the pitch-based carbon obtained by using silica colloidal crystal as template.[10] Ryoo's group first synthesized ordered mesoporous carbon with graphitic framework structures through in situ conversion of an aromatic compound, acenaphthene, to mesophase pitch inside the silica templates.[11] However, for uses in catalysis, the structural mesoscale ordering is in most cases not necessary.

The synthetic processes discussed above either require high temperatures or are rather time-consuming, and in most cases cannot be applied for economical and large-scale production. Therefore, the exploration of simple and scalable synthetic procedures for graphitic, highly porous carbons is an interesting task. Up to now, the synthesis of porous graphitic carbon with high surface area and structural ordering at low temperature is still a great challenge. In the present study, we report the synthesis of high surface area graphitic carbon by pyrolysis cobalt-containing polymer particles in which the cobalt is atomically dispersed. The evolution of the graphitic structure together with substantial mesoporosity is temperature dependent. This effect can be better followed in the present case than for carbon aerogels.[5e,6] Moreover, the use of silica as an isolating shell facilitates the formation of high surface area graphitic carbon.

2. Experimental Section

2.1. Synthesis Procedure. The carbon precursor, 1.75 g of dihydroxybenzoic acid ($C_7H_6O_4$, 98%, Fluka), was dissolved in water in the presence of Na_2CO_3 (98%, Fluka) with the $C_7H_6O_4$ to Na_2CO_3 molar ratio of 2:1 to form a clear, light orange colored solution. After the addition of formaldehyde (37%, Fluka, the molar ratio of dihydroxybenzoic acid to formaldehyde was fixed as 1:2), the solution was maintained at 80 °C for 24 h, and subsequently, 1.5 g of surfactant CTAB (98%, ACROS) was added to the solution, resulting in precipitation. The mother solution was aged at 90 °C for 2 days. The precipitate was collected by filtration and washing. After drying, the obtained polymer particles were immersed in a cobalt nitrate solution with a concentration of 0.25 M under stirring at 50 °C for 12 h. Afterward, the polymer particles were collected by filtration and washed intensively to remove the nonexchanged cobalt cations. Subsequently, the Co^{2+}-containing polymer particles were heated to 150 °C for 4 h under an argon atmosphere and then heated to 300 °C with a heating ramp of 1 °C/min. Finally, the temperature was increased to the desired temperature with a heating ramp of 5 °C/min and maintained at this temperature for 2 h. The obtained carbon/cobalt composites were denoted as GC(*x*), where *x* indicates the pyrolysis temperature. To introduce oxygen-containing functional groups on the surface of the carbon and to remove cobalt, these samples were further treated with 53% of nitric acid for 24 h at 60 or 100 °C. The carbon product was recovered after filtration, washing with water and ethanol, and drying at 90 °C. The resulting porous carbons are denoted as GC(*x*)-*y*, wherein *x* and *y* indicate the temperatures of pyrolysis and nitric acid oxidation, respectively. The carbon yields are usually in the range of 30−40 wt % based on the mass of the starting polymer. For comparison, polymer which had not been subjected to cobalt exchange was carbonized at the same conditions to examine the structural difference. This sample was denoted G(*x*).

2.2. Characterization. The samples were characterized by X-ray diffraction (XRD), nitrogen sorption measurements, high-resolution electron transmission spectroscopy (HRTEM), and so forth. XRD patterns of all the samples were recorded with a STADI P diffractometer (Stoe) in the Bragg−Brentano (reflection) geometry. Nitrogen adsorption isotherms were measured with an ASAP2010 adsorption analyzer (Micromeritics) at liquid nitrogen temperature. Prior to the measurements, the samples before and after removal of cobalt particles were degassed at a temperature of 150 °C for 6 h. All materials contained micropores, which prevents a proper determination of their specific surface areas by the BET method. Thus, only apparent surface areas are given, which were calculated from the adsorption data in the relative pressure intervals from 0.04 to 0.2 using the BET method. Pore size distribution (PSD) curves were calculated by the BJH (Barrett−Joyner−Halenda) method from the adsorption branch. The desorption branch which is normally recommended was not used, because the closure of the hysteresis loop at the capillary critical point of $p/p_0 = 0.42$ could lead to artifacts for several of the samples. Thermogravimetic analysis (TGA) was performed on a NETZSCH STA 449C thermobalance. The measurement was carried out under air with a heating rate of 10 °C/min. TEM images were obtained with a HF2000 microscope (Hitachi), equipped with a cold field emission gun. The acceleration voltage was 200 kV. Samples were prepared on a lacey carbon grid. The IR spectra of acid oxidized carbons were collected on a Magna-IR 750 Nicolet Fourier transform infrared (FTIR) spectrometer. The samples were prepared as KBr wafers, measured from 4000 to 400 cm^{-1}. As a supplement, the graphitic carbon/cobalt composites have been characterized by a superconducting quantum interference device (SQUID) magnetometry to investigate the magnetic properties.

(5) (a) Moreno-Castilla, C.; Maldonado-Hódar, F. J.; Carrasco-Marín, F.; Rodríguez-Castellón, E. *Langmuir* **2002**, *18*, 2295. (b) Maldonado-Hodar, F. J.; Perez-Cadenas, A. F.; Moreno-Castilla, C. *Carbon* **2003**, *41*, 1291. (c) Baumann, T. F.; Fox, G. A.; Satcher, J. H., Jr.; Yoshizawa, N.; Fu, F.; Dresselhaus, M. S. *Langmuir* **2002**, *18*, 7073. (d) Bekyarova, E.; Kaneko, K. *Adv. Mater.* **2000**, *12*, 1625. (e) Maldonado-Hodar, F. J.; Ferro-García, M. A.; Rivera-Utrilla, J.; Moreno-Castilla, C. *Carbon* **1999**, *37*, 1199.
(6) Fu, R.; Baumann, T. F.; Cronin, S.; Dresselhaus, G.; Dresselhaus, M. S.; Satcher, J. H., Jr. *Langmuir* **2005**, *21*, 2647.
(7) Maldonado-Hodar, F. J.; Moreno-Castilla, C.; Rivera-Utrilla, J.; Hanzawa, Y.; Yamada, Y. *Langmuir* **2000**, *16*, 4367.
(8) Hyeon, T.; Han, S.; Sung, Y.-E.; Park, K.-W.; Kim, Y.-W. *Angew. Chem., Int. Ed.* **2003**, *42*, 4352.
(9) Lu, A.-H.; Li, W.; Matoussevitch, N.; Spliethoff, B.; Bönnemann, H.; Schüth, F. *Chem. Commun.* **2005**, 98.
(10) Yoon, S. B.; Chai, G. S.; Kang, S. K.; Yu, J.-S.; Gierszal, K. P.; Jaroniec, M. *J. Am. Chem. Soc.* **2005**, *127* (12), 4188.
(11) Kim, T.-W.; Park, I.-S.; Ryoo, R. *Angew. Chem., Int. Ed.* **2003**, *42*, 4375.

3. Results and Discussion

3.1. Preparation of Porous Graphitic Carbon. It is known that the solid content (ratio of polymer to solvent) plays an important role in directing the polymerization process toward a polymer gel or polymer nanoparticles. The first aim of this work is to find the synthetic conditions where polymer nanoparticles instead of polymer gel can be prepared through wet chemistry. Therefore, the solid content, that is, weight ratios of $C_7H_6O_4$ and formaldehyde to water, were varied from 0.8 to 10%. To dissolve $C_7H_6O_4$ in water, Na_2CO_3 is needed to ionize the carboxyl group which results in the formation of a clear solution. Polymer particles were formed after addition of formaldehyde at the reaction temperature of 80 °C. With water as the solvent, the solution maintains the homogeneous liquid phase with a wine color, as long as the solid content stays lower than 4 wt %; when the solid content increases above 5 wt %, the solution will become gel. However, by adding ethanol as the cosolvent, the solid content can be increased to 6 wt % until gelation occurs; below this value, the solution is clear and transparent. Light scattering analysis shows that at a solid content of 3 wt % and with water as the solvent, the polymer particles are in the size range of 50 nm. Longer reaction times result in agglomeration of the particles, which can be redissolved in ammonia solution. At a solid content of 4 wt % and with water/ethanol as the solvent, the polymer particles can be prepared with a size of 120−210 nm, depending on the reaction time. Considering the requirement to produce polymer nanoparticles and achieve a reasonable yield for one reaction batch, we mainly investigated the polymer prepared at a solids content of 4 wt % in the following experiments.

To collect these nanoparticles, a certain amount of surfactant CTAB was added to the solution, resulting in precipitation. After aging, the precipitate was collected by filtration and washing with distilled water. The particles were ion exchanged with Co^{2+} solution, and the polymer particles were subjected to pyrolysis under an argon atmosphere. The obtained samples were characterized with XRD to identify the phases; pyrolysis at 700 °C leads to the formation of amorphous material, for both GC(700) and GC(700)-80 and before and after cobalt leaching (Figure 1). No reflections which could be assigned to a cobalt phase are visible. This indicates that the cobalt particles are either very small below the detection limit of the XRD, or the reflections are hidden by the background of the amorphous phase. In contrast, the XRD patterns of samples pyrolyzed at temperatures exceeding 850 °C show well-resolved reflections. For example, in the XRD pattern of GC(850) clear reflections can be assigned to graphitic carbon and metallic cobalt. After treatment with nitric acid, the reflections corresponding to the metallic cobalt disappear, and only the reflections assigned to graphite remain, as can be seen for sample GC(850)-80, indicating that graphitic carbon is obtained at a pyrolysis temperature of 850 °C. Samples subjected to a pyrolysis temperature of 1000 °C also show well-developed graphitic structure after acid treatment, as reflected in the XRD pattern in Figure 1. Only heating the same polymer particles without cobalt cations to 850 °C leads to formation of amorphous material, as reflected in the XRD pattern of G(850), indicating that

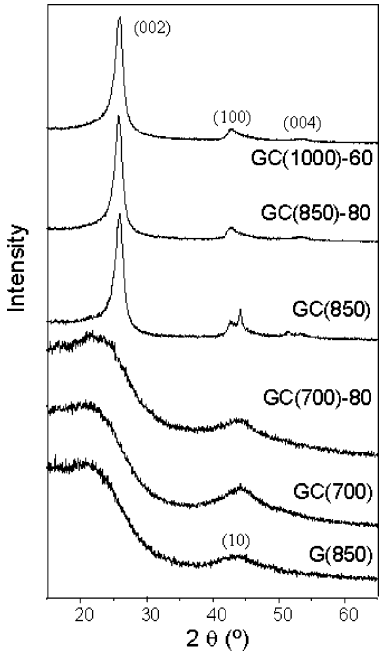

Figure 1. XRD patterns of graphitic carbons synthesized at different conditions. For sample codes, see Experimental Section.

the presence of cobalt is crucial for the formation of graphitic carbon. By combining the above results, it is clear that the formation of the graphitic structure is facilitated by the presence of cobalt catalyst and is dependent on temperature. When the ion exchange process is used, the cobalt catalyst is dispersed homogeneously throughout the polymer particles, as revealed by the energy-dispersive X-ray (EDX)−TEM analyses. This is advantageous compared to the mechanical mixing method of cobalt salt and carbon precursor. The results demonstrate that graphitic carbon with a high graphitization degree can be obtained at a low pyrolysis temperature of 850 °C, which is much lower than 2000 °C, the temperature normally required for the preparation of graphite carbon.

The nitrogen sorption isotherms of the samples are shown in Figure 2a, and the textural parameters are compiled in Table 1. The isotherms of samples pyrolyzed at temperatures exceeding 850 °C show type IV character with a clear hysteresis loop in the relative pressure range of 0.4−0.8, indicating their mesoporous characteristics. After nitric acid treatment, specifically when the temperature during the acid treatment increases to 100 °C, the isotherm of GC(850)-100 retains an identical shape, but with obviously increased nitrogen uptake, indicating that pore opening occurs. The isotherm of sample GC(1000) pyrolyzed at 1000 °C is almost identical in shape compared to that of GC(850), indicating that the graphitic structures formed at 850 °C are already stable and that almost no sintering effect occurs. Similarly, also the acid treatment for GC(1000) leads to an increase in the adsorbed volume of sample GC(1000)-60. The apparent surface areas of these carbons decrease after nitric acid treatment. However, the total pore volumes increase, as a result of the fact that the removal of cobalt nanoparticles leaves some spaces which are in the detectable range of nitrogen sorption. The decrease in the BET surface area and the changes in pore structure brought about by strong

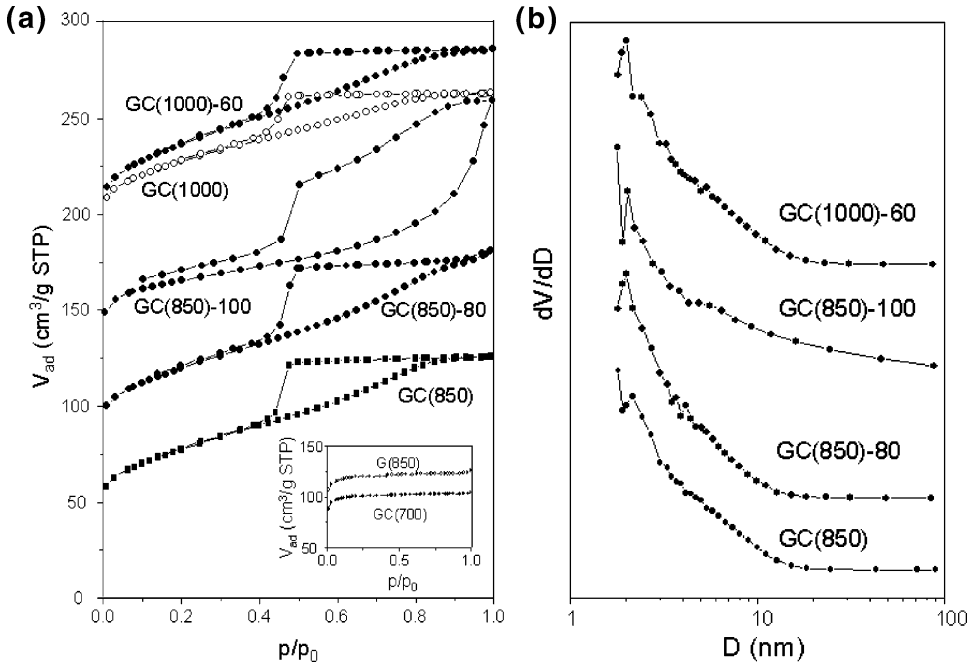

Figure 2. Nitrogen sorption isotherms (a) and PSDs (b) of graphitic carbons synthesized at different conditions. The isotherms of GC(850)-80, GC(850)-100, GC(1000), GC(1000)-60, and G(850) are offset vertically by 50, 125, 150, 150, and 25 cm^3 g^{-1} STP, respectively.

Table 1. Texture Parameters of Graphitic Carbon/Cobalt Composites and Graphitic Carbons[a]

sample	Py (°C)	NA (°C)	S_{BET} (m^2 g^{-1})	V_{tot} (cm^3 g^{-1})
G(850)	850		319	0.153
GC(700)	700		338	0.160
GC(700)-80	700	80	0.9	0.001
GC(850)	850		266	0.192
GC(850)-80	850	80	245	0.199
GC(850)-100	850	100	141	0.205
GC(1000)	1000		267	0.174
GC(1000)-60	1000	60	299	0.208
*GC(850)	850		280	0.187
*GC(850)−80	850	80	278	0.230
GC-A	1000		303	0.276
GC-B[b]	1000	80	470	0.535

[a] Note: Py, pyrolysis temperature; NA, oxidation temperature of nitric acid; S_{BET}, apparent surface area calculated by the BET method; V_{tot}, total pore volume at $p/p_0 = 0.9$. [b] Sample first treated with NaOH aqueous solution and then HNO_3 solution.

oxidants may be attributed to some destruction of the pore walls. Nitric acid at high concentration produces a destruction of the pores. Moreover, the pore walls may collapse when oxygenated terminal groups are created. It is generally assumed and reported that relatively mild liquid phase oxidations do not change significantly the texture of the activated carbons,[12] although under more drastic conditions a decrease in surface area and pore volume has been observed while the average micropore width increases, due to the collapse of the pore walls.[13] For the ordered carbon CMK-5, even complete structural disintegration has been reported after treatment with hydrogen peroxide.[14] The calculated PSDs of all the samples are shown in Figure 2b. Basically, for all samples the pores are located predominantly in the lower mesopore/supermicropore range, with an apparent maximum around 2.2 nm. However, because the BJH algorithm is not fully appropriate for this size range, this number should be interpreted with caution. The high temperature of nitric acid treatment results in the development of pores around 5−6 nm, indicated by a shoulder of the PSD of sample GC(850)-100. This might be due to the contribution of pores generated during the removal of cobalt nanoparticles. It is noteworthy that pyrolysis at 700 °C of the same polymer particles containing cobalt cations did not result in the formation of any mesoporosity; the resulting carbon is rather microporous with a type I isotherm (inset in Figure 2a), and the apparent surface area is 338 m^2/g. Similarly, the same polymer particles without cobalt cations were pyrolyzed at 850 °C to result in carbon G(850), which also shows a type I isotherm corresponding to a microporous material (inset in Figure 2a). It is well-known that microporosity is usually generated during pyrolysis of a polymer. After nitric acid treatment at 80 °C, the sample GC(700) loses almost all porosity, suggesting that the microposity might be destroyed by acid oxidation through the formation of an oxygen-containing group which could block the micropore entrances. From the textural data, one can conclude that during pyrolysis at 700 °C, cobalt cations are not able to form big cobalt clusters (this will be further discussed in the TEM characterization). Otherwise, the removal of cobalt particles should have resulted in accessible porosity which would be detectable by nitrogen sorption. The above results clearly prove that mesopores in graphitic carbon were generated as a result of the influence of both the existence of cobalt nanoparticles and suitable pyrolysis temperature (at least 850 °C). At these temperatures cobalt nanoparticles also catalyze the formation of the graphitic nanostructure. According to the TGA results, the metallic cobalt content is about 4.4 wt % (calculated from 6.1 wt % of Co_3O_4), which is too little to explain the formation of mesopores, if each cobalt particle would be acting only as a

(12) Noh, J. S.; Schwarz, V. *Carbon* **1990**, *28*, 675.
(13) Moreno-Castilla, C.; Carrasco-Marín, F.; Maldonado-Hódar, F. J.; Rivera-Utrilla, J. *Carbon* **1998**, *36*, 145.
(14) Lu, A.-H.; Li, W.; Muratova, N.; Spliethoff, B.; Schüth, F. *Chem.* Commun. **2005**, 5184.

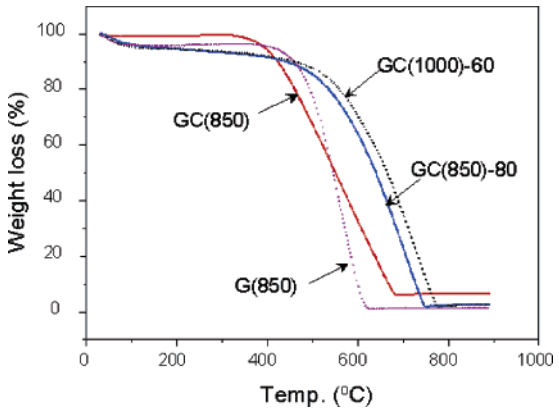

Figure 3. TGA curves of samples GC(1000)-60, GC(850)-80, GC(850), and G(850).

porogene. Therefore, the porosity must be formed by continuously cobalt nanoparticle catalyzed carbonization at high temperatures above 700 °C, similar to the effect of carbon nanotube formation. This effect will be better understood by the TEM investigations as discussed further below.

It is generally accepted that graphitized carbons with a higher graphitization degree are more stable against air oxidation. To study the resistance of our carbons, TGA analyses were performed for the obtained samples under air to examine the oxidation behavior of these porous carbons. As seen in Figure 3, pure carbon G(850) is more rapidly oxidized compared to the graphitic samples; that is, the amorphous carbon is more easily oxidized with oxygen. This is also the reason graphitic carbon is difficult to activate by gas oxidation. It is necessary to point out that cobalt-containing graphitic carbon GC(850) is more easily oxidized at temperatures below 550 °C compared to the pure carbon G(850). This might be due to the catalytic oxidation by metallic cobalt nanoparticles, which are accessible by oxygen molecules and catalyze graphitic species into CO_2 at lower temperature; simultaneously (gradually), metallic cobalt species are converted to oxides with reduced catalytic activity. High temperature prepared graphitic carbon GC-(1000)-60 shows better oxidation resistance than the one prepared at lower temperature GC(850)-80, which is due to the different graphitization degree of these samples.

For comparison, graphitic carbon was also prepared with a higher loading of cobalt. The temperature of pyrolysis was kept at 850 °C, and the nitric acid treatment was performed at 80 °C. The samples before and after acid treatment are denoted as *GC(850) and *GC(850)-80, respectively. TGA (Figure 4a) shows that 9.8 wt % of cobalt oxides are left in this graphitic carbon *GC(850), which corresponds to 7.1 wt % of metallic cobalt, assuming Co_3O_4 as the oxide. XRD patterns (Figure 4b) reveal that the obtained carbon still essentially has a similar graphitization degree but with clearly distinguishable reflections assigned to metallic cobalt, corresponding to a relatively large particle size. This indicates a higher tendency toward sintering for cobalt particles at high cobalt loading. After the treatment with nitric acid, the reflections assigned to cobalt disappear, and only the reflections belonging to the graphitic structure are observed,

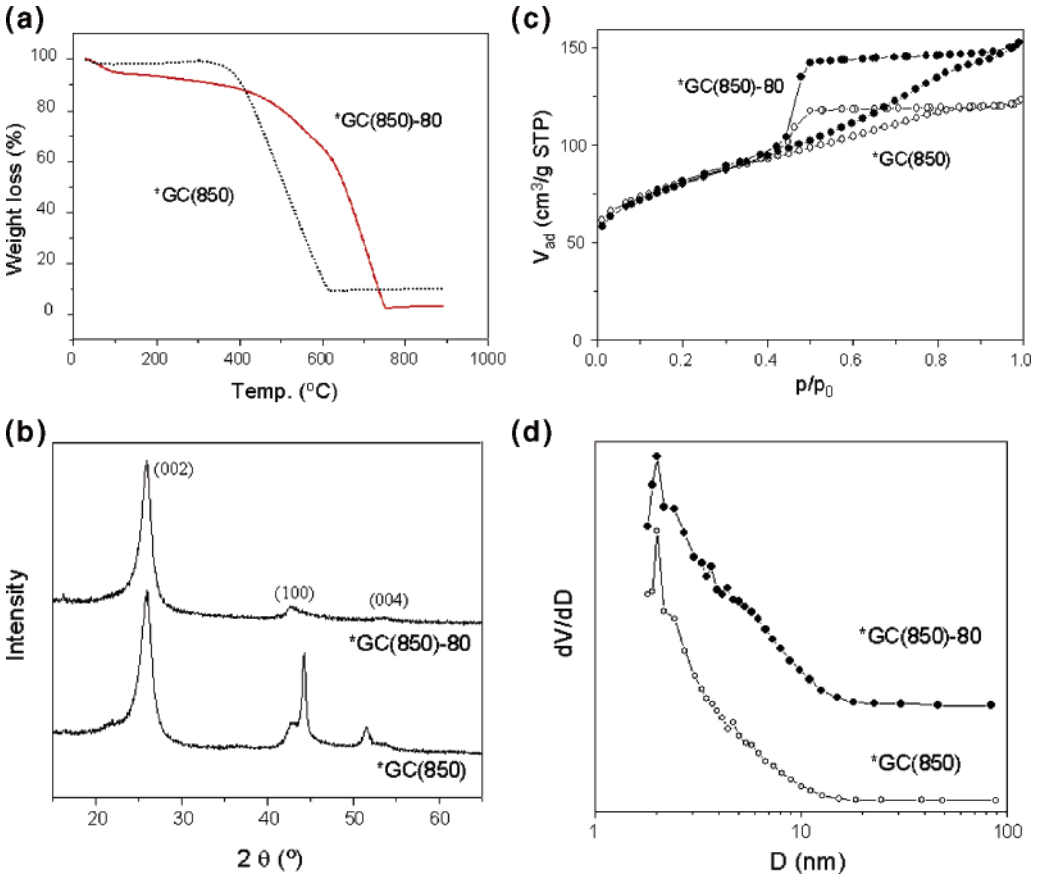

Figure 4. TGA curves (a), XRD patterns (b), nitrogen sorption isotherms (c), and PSDs (d) of graphitic carbon prepared at high cobalt loading. The asterisk indicates the high loading, and the rest of the codes are the same as for other samples.

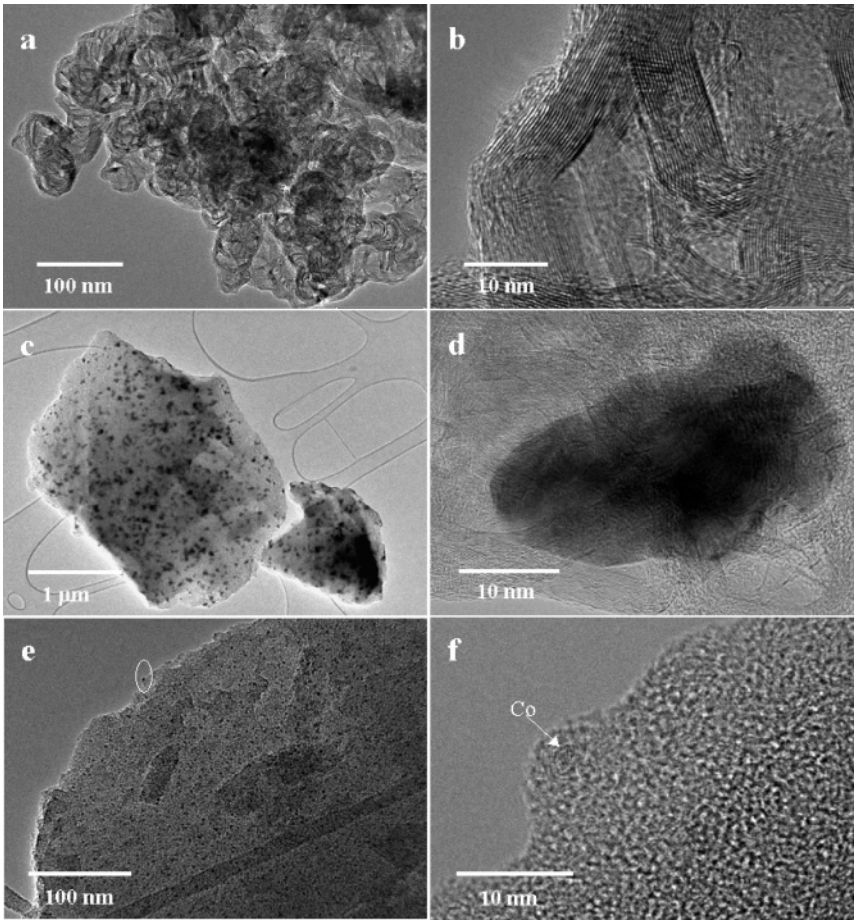

Figure 5. TEM images of graphitic carbon GC(850)-100 (a, b), *GC(850) (c, d), and GC(700) (e, f).

indicating the complete removal of the cobalt nanoparticles by acid treatment even at high cobalt loading. Nitrogen sorption isotherms (Figure 4c) are of type IV, indicative of mesopores, similar to that of the GC(850) carbon. Again, the removal of cobalt nanoparticles leads to an increase of the adsorbed volume of *GC(850)-80. Both samples have a narrow PSD around 2.2 nm (Figure 4d), and the nitric acid treatment resulted in the development of pores around 5−6 nm, which can be seen from the shoulder in the PSD of this sample. However, with respect to the textural data, the numerical values should be treated with caution, as discussed above.

To obtain more detailed structural insight, the samples were investigated by TEM analysis (Figure 5). The sample GC(850)-100, pyrolyzed at 850 °C and washed with nitric acid at 100 °C, essentially shows a well-developed turbostratic graphite structure (Figure 5a). Cobalt concentrations in the nitric acid oxidized graphitic carbon are below the detection level of EDX analysis, proving the effectiveness of the nitric acid washing step. At high resolution (Figure 5b), a thin layer of amorphous carbon on the outer surface of the graphitic carbon is discernible, probably as a result of the erosion effect of nitric acid. This is expected, because the purpose of the acid oxidation is not only removal of the cobalt particles but also opening of the closed pores, as reflected from the nitrogen sorption analyses. To understand how the cobalt particles are distributed in the carbon materials, the sample *GC(850), prepared at high cobalt loading, was investigated by TEM. As seen in Figure 5c, cobalt particles with sizes of tens of nanometers are uniformly distributed throughout the entire carbon particles. The graphitized structure of this sample can be clearly observed in Figure 5d at high resolution. Not a single amorphous carbon cluster can be found, indicating the high graphitization degree and homogeneity of this cobalt catalyzed graphitized carbon. As discussed above, GC(700) shows amorphous and microporous characteristics. To monitor the state of the cobalt species, this sample was also analyzed by TEM. Cobalt particles with the size of about 2 nm are present in the carbon matrix, which are homogeneously dispersed through the entire sample (Figure 5e). As shown in Figure 5f, the cobalt particles are crystalline, exhibiting lattice fringes. However, the carbon matrix is amorphous, which corroborates the XRD result that, at 700 °C, the small cobalt particles do not induce graphitization of the carbon. Incidentally, however, this observation provides a recipe for the generation of highly dispersed cobalt particles in a carbon matrix, which may be generalizable to other transition metals. By comparing the above TEM analyses, one can conclude that the cobalt species do not have any catalytic effect at temperatures below 700 °C. With the increase of the temperature from 700 to 850 °C, the cobalt nanoparticles start to grow and simultaneously and continuously catalyze the conversion of the amorphous carbon matrix to form graphitic carbon. This process occurs within a rather narrow temperature window and relatively short period.

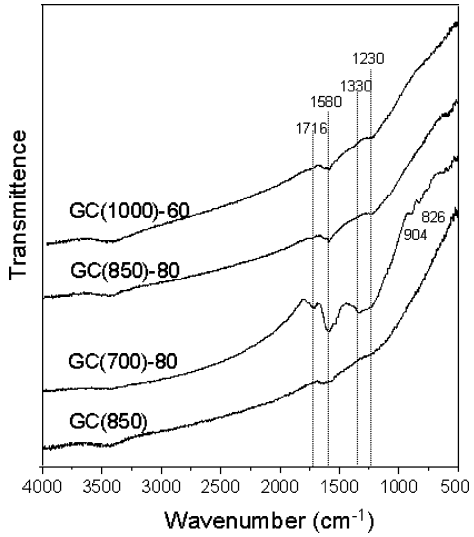

Figure 6. FTIR spectra of graphitic carbons before and after acid treatment.

FTIR spectroscopy was used to detect the development of the surface functional groups of graphitic carbon during nitric acid oxidation, and the corresponding FTIR spectra of carbons before and after acid treatment are shown in Figure 6. After acid oxidation, one can see remarkable changes in the spectra as compared to the original one (GC(850)). Several new bands are present at 1716, 1580, and 1338 cm^{-1}, associated with shoulders close to these new bands. GC-(700)-80 shows more intense and more clearly resolved bands than the carbons obtained at higher pyrolysis temperature. This is due to the amorphous structure of GC(700) which is more easily oxidized with nitric acid than graphitic carbon. The band around 3412 cm^{-1} is attributed to the —OH groups in the graphitic carbon. FTIR peaks appearing around 1720 cm^{-1} can be assigned to the C═O stretching vibrations from ketones or carboxyl groups. The band at 1230 cm^{-1} can be assigned to C—O—C vibrations in ether structures. These results indicate that there are some changes of the graphitic carbon during oxidation with nitric acid. It is assumed that these functional groups are predominantly present on the external surface of the graphitic carbon, which is also indicated by the thin amorphous layer seen in HRTEM.

The advantage of the synthetic pathway used in this study is the fact that cobalt cations are homogeneously dispersed throughout the entire polymer particle. This is due to the uniform distribution of carboxyl groups within such a polymer. However, sintering of the particles still takes place during pyrolysis. To prevent this sintering, the synthesis of a protective layer on the polymer particles seems to be a viable approach. Silica seems to be suitable for this; as it is widely used in nanocasting processes, the silica-protecting layer could be easily dissolved by the NaOH solution in the end.[15] To test this idea, one batch of as-prepared polymer particles was added into a tetraethyl orthosilicate solution, using ammonia as the hydrolysis catalyst (Stöber process). To obtain well-dispersed nanosized polymer particles coated with silica, a lower solid content (1.2% ratio of polymer to water) was selected. The sample after this step is obtained as a very fine powder. This sample was further treated by ion exchange with cobalt nitrate, followed by filtration, washing, drying, and pyrolysis at 1000 °C to produce the silica/carbon/cobalt composite denoted GC-A. This composite was treated with NaOH aqueous solution at 80 °C for 2 days to dissolve the silica layer, followed by nitric acid treatment at 80 °C for 24 h to remove the cobalt particles. The obtained sample, denoted as GC-B, was characterized by TGA, XRD, and nitrogen sorption measurements. The TGA result of GC-B shows that the ash content is about 0.2 wt %, indicating that nearly complete removal of cobalt and silica had taken place. Comparing to pure carbon, GC-B shows better oxidation resistance. While the pure carbon is completely combusted at 620 °C, GC-B still has nearly half of the weight left at this temperature. This oxidation

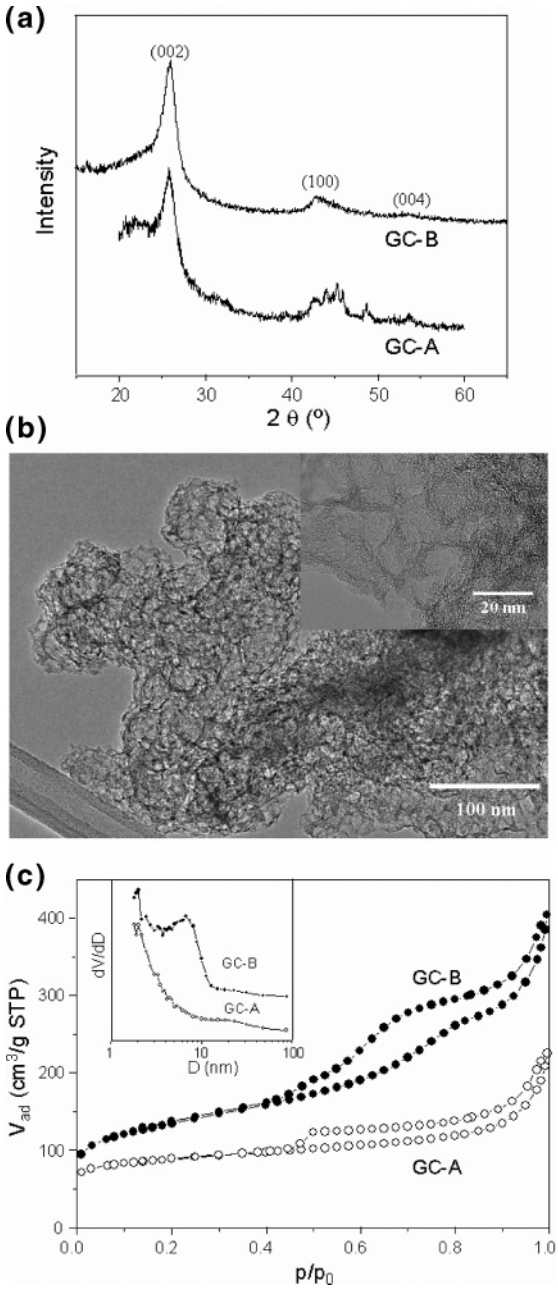

Figure 7. XRD patterns (a), TEM images (b), nitrogen sorption isotherms (c), and PSDs (c, inset) of graphitic carbons prepared under the protection of a layer of silica. Samples are labeled as GC-A (before acid treatment) and GC-B (after acid treatment).

(15) (a) Lu, A.-H.; Schüth, F. *C. R. Chim.* **2005**, *8* 609. (b) Yang, H.; Zhao, D. *J. Mater. Chem.* **2005**, *15*, 1217.

resistance is due to the very well-developed graphitic structure. The XRD pattern of GC-A (Figure 7a) shows reflections for the graphitic phase and cobalt as well as other unidentified phases. After the treatment with NaOH aqueous solution and nitric acid solution, respectively, the XRD pattern of GC-B clearly shows the existence of the graphite phase, and probably some amorphous material is present as well, according to a relatively high baseline between 20 and 30°. The TEM image in Figure 7b reveals that this sample has abundant porosity in the mesopore range. Differing from the structure of GC(850), sample GC-B exhibits very thin carbon walls, as seen from the HRTEM image (Figure 7b, inset). The carbon framework consists of nanosized graphitic domains, enclosing pores with sizes in the range of 7−10 nm. Thus, the results from XRD and TEM are consistent with each other. It is obvious that the difference between GC(850) and GC-B is mainly due to the addition of silica during the polymer synthesis and higher graphitization temperature.

The nitrogen sorption isotherms of GC-A and GC-B are presented in Figure 7c. Both samples exhibit type IV isotherms with hysteresis loops, characteristic for mesoporosity. After leaching of silica and cobalt, the mesopore feature of GC-B is becoming more pronounced, as can be inferred from the substantial uptake in the pressure region above 0.5 and the well-developed hysteresis. Additional pronounced pores with sizes of around 6.5 nm appear after leaching in sample GC-B (Figure 7c, inset). As seen in Table 1, the BET surface area and, especially, the total pore volume of GC-B are remarkably high, due to the removal of silica and cobalt. This method may provide a synthetic pathway for the preparation of high surface area porous graphitic carbon with small graphitic domains, which are considered as a possible compromise between good electronic conductivity and high surface area.

3.2. Magnetic Properties of the Graphitic Carbon/Cobalt Composite. XRD and TEM results of the cobalt-containing samples described above show that the cobalt particles are crystalline. It would be interesting to know how stable these cobalt nanoparticles embedded in graphite shells are. In the following, the magnetic properties of these materials together with their magnetic stability were investigated.

Magnetic hysteresis loops measured at 300 and 5 K for GC(850) and *GC(850) are shown in Figure 8. Both samples are ferromagnetic, reaching saturation in magnetic fields of around 1 T. Temperature dependent values of the coercivity (H_c), saturation (M_s), and remanent (M_r) magnetization are listed in Table 2. The long-range magnetic order present in this system of carbon/cobalt nanoparticles is stabilized by the dipolar coupling between the particles. An estimate of the dipolar energy between two particles with an effective magnetic moment of $5 \times 10^5\ \mu_B$, by assuming that all the particles possess the same magnetic moment aligned along the same axis, and located at a distance of 100 nm apart from each other yields 2×10^{-21} J (12 meV). This large value of the dipolar strength explains very well the magnetic order measured even at room temperature. As a result of the fact that each cobalt nanoparticle is surrounded by a graphite shell with a thickness in the range of 10−20 nm, the presence of an exchange interaction between Co nanoparticles can be ruled out. A smaller cobalt particle size for the sample GC(850) leads to a reduction of the saturation magnetization and coercivity. As expected, the temperature dependence of the magnetization curves (zero-field and field-cooled in an applied field of 5 T) reveals no superparamagnetic behavior below room temperature (data not shown). The magnetic stability for sample *GC(850) was checked again over a time of 10 months. No degradation of the magnetic properties was observed which proves that the cobalt particles are well-protected against oxidation in air by the graphite matrix.

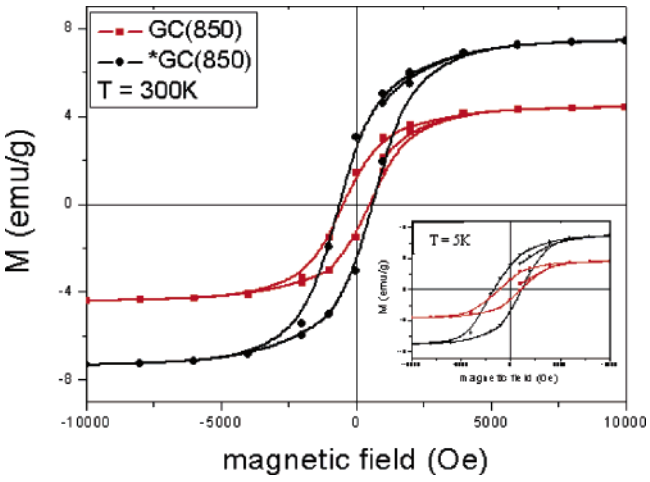

Figure 8. Magnetic hysteresis curves for the graphitic carbon/cobalt composites recorded at 300 and 5 K (in the inset).

Table 2. Summary of Magnetic Properties of Graphitic Carbon/Cobalt Composites

	$T = 5$ K			$T = 300$ K		
sample	H_c (kA/m)	M_s (A m^2/kg)	M_r (A m^2/kg)	H_c (kA/m)	M_s (A m^2/kg)	M_r (A m^2/kg)
*GC(850)	114	8.9	3.8	48	7.4	3
GC(850)	79	4.6	1.5	38	4.3	1.4

An interesting feature of the carbon/cobalt nanoparticles was extracted from the field-cooled (in a magnetic field of 5 T) hysteresis curves taken at $T = 5$ K (data not shown). Usually, one expects an oxide layer around each cobalt nanoparticle which can lead to an exchange coupling between the ferromagnetic Co core and the antiferromagnetic CoO or Co_3O_4 shell, called the exchange bias effect.[16] This effect is visible as a shift of the field-cooled hysteresis loop on the magnetic field axis. In the present case, no shift of the field-cooled hysteresis loops was observed. The lack of the exchange coupling between the ferromagnetic core and the antiferromagnetic shell indicates that the Co nanoparticles are not surrounded by an oxide layer or the oxide layer is very thin (less than 2 nm). The presence of an about 2 nm thick antiferromagnetic shell will lead to a measurable exchange bias.[17] This measurement shows that the cobalt particles exist in the metallic state instead of the oxidic state in graphitic carbon. Moreover, these metallic cobalt particles

(16) Noques, J.; Schuller, I. K. *J. Magn. Magn. Mater.* **1999**, *192*, 203.
(17) Spasova, M.; Wiedwald, U.; Farle, M.; Radetic, T.; Dahmen, U.; Hilgendorff, M.; Giersig, M. *J. Magn. Magn. Mater.* **2004**, *272−276*, 1508.

are very stable in air because of the protection by the graphitic carbon.

4. Conclusion

High surface area graphitic carbon has been prepared through polymer synthesis, ion exchange, and pyrolysis. Cobalt nanoparticles play an important role in the catalytic formation of the graphitic nanostructure that is temperature dependent. Nitric acid oxidation can completely remove the cobalt nanoparticles at low temperature and leave the pore system open. Magnetization measurements show that the graphitic carbon/cobalt composites exhibit ferromagnetic properties and that the cobalt nanoparticles are stable in air for more than 10 months without degradation of the magnetic properties, which proves the excellent protection of the cobalt particles by the graphitic carbon shell.

Acknowledgment. The authors would like to thank Mr. Goebels for SQUID measurements, the DFG for funds provided by the Leibniz-program, in addition to the basic funding from the Institute.

CM060135P